Eur. Phys. J. D **9**, 303–307 (1999)

THE EUROPEAN PHYSICAL JOURNAL D
EDP Sciences

Photoelectron spectroscopy of 7-azaindole–water cluster anions

A. Nakajima, Y. Negishi, R. Hasumi, and K. Kaya

Department of Chemistry, Faculty of Science and Technology, Keio University, 3-14-1 Hiyoshi, Kohoku-ku, Yokohama 223-8522, Japan

Received: 31 August 1998 / Received in final form: 15 December 1998

Abstract. The 7-azaindole (7-AzI) cluster anions and their H_2O adducts were generated by electron attachment to the 7-AzI/7-AzI–H_2O clusters, and their electronic properties studied with mass spectrometry and photoelectron spectroscopy. In the mass spectra of the 7-AzI cluster anions, $(\text{7-AzI})_n^-$, monomer anions were missing due to negative electron affinity (EA), while clusters ($n \geq 2$) have positive EA, and those having even n were more abundant than those at odd n. EA increased with cluster size from 0.88 eV at $n = 2$, and an even–odd alternation in the EA was seen. The even–odd alternation showed that the 7-AzI dimer acts as a unit for cluster formation. In the photoelectron spectrum of $(\text{7-AzI})_2^-$ at 266 nm, the second peak was observed 2.4 eV above the first peak; this is attributed to the triplet state of the neutral $(\text{7-AzI})_2$. Depending on the detachment energy, a movable peak, with the detachment of 420–300 nm (2.9–4.1 eV), was additionally observed between the first and the second peaks; this was thought to be caused by a delayed photoemission via an electronic excited state of the $(\text{7-AzI})_2^-$ anion.

PACS. 36.40.-c Atomic and molecular clusters – 82.30.Nr Association, addition, insertion, cluster formation, hydrogen bonding – 71.24.+q Electronic structure of clusters and nanoparticles

1 Introduction

Proton-transfer reactions (PTR) are fundamentally important reactions playing an important role in a variety of chemical and biological processes [1–3]. Among many molecules undergoing this type of photoreaction, a dimer of 7-azaindole (7-AzI) particularly deserves much attention, because it exhibits a well-documented example of cooperative double PTR in its excited state [4–15]. However, there has been hardly any spectroscopic study about the electronic and geometric structures of the 7-AzI dimer in the gas phase. The recent development of tunable, ultraviolet, high-resolution dye lasers has indeed opened up a new region of the spectrum to high-resolution studies [16, 17]; this enables us to investigate the geometric structures of complexes between aromatic molecules and waters with fully resolved rotational spectroscopy [18, 19]. For 7-azaindole–water complexes, $(\text{7-AzI})\text{-}(H_2O)_n$ ($n = 1-3$), we have investigated the geometric structures by laser-induced fluorescence (LIF) spectroscopy with high resolution ($\sim 0.01\,\text{cm}^{-1}$) [20]. However, a very fast PTR often gives an unresolved rotational envelope, following the uncertainty principle, and one of the examples involving the very fast PTR is the 7-AzI dimer [15].

Recently, photoelectron spectroscopy for cluster anions has been proven to be a powerful technique for studying the electronic and geometric structures of atomic/molecular clusters in gas phase as a function of size [21, 22], due to its ability to combine size selectivity with quantitative spectral sensitivity. Since photodetachment is a process of transition from the ground state of anions into the ground state or electronic excited states of the corresponding neutrals, the electronic properties of the neutral clusters are therefore readily observed from the photoelectron spectra. It is generally possible to derive information on the bonding nature, and thus the geometry, of the clusters from the analysis of photoelectron spectra.

Furthermore, the geometric structure of 7-AzI clusters intrigues us, because it is capable of self-associating through hydrogen bonds [23, 24]. Since a 7-AzI cluster has both donor and acceptor sites for hydrogen bonding, the geometric arrangements can lead to the formation of cyclic structures and/or open-chain structures. When H_2O molecules are added, the network structures of hydrogen bonding are deformed because of additional hydrogen bondsl; this is closely related to microscopic solvation behavior.

In this paper, we report electronic and geometric structures of 7-AzI and 7-AzI–H_2O clusters studied by mass spectrometry and photoelectron spectroscopy. In the photoelectron spectrum of $(\text{7-AzI})_2^-$, the excitation into the triplet excited state of the neutral $(\text{7-AzI})_2$ was identified and a movable peak, which depends on the detachment wavelength, was found. Moreover, the most probable geometric structure for 7-AzI–H_2O clusters was obtained by these methods and will be discussed from the viewpoint of microsolvation.

2 Experimental

The details of the experimental setup have been provided elsewhere [24]. Briefly, the apparatus consists of a pulsed cluster anion source, a time-of-flight (TOF) mass spectrometer, and a magnetic bottle TOF spectrometer. Under a supersonic expansion of 7-AzI in a He carrier gas ($\sim$10 atm), 7-AzI cluster anions were formed by two methods: either (1) injection of electrons having slow kinetic energy or (2) pulsed discharge for the expansion [25]. In the former method, the electrons were produced by the focus of the second harmonics of an Nd^{3+}:YAG laser (Quanta-Ray, GCR-12) gently onto a Y_2O_3 disk surface located at $\sim$ 4 mm downstream from a pulsed valve (400-μm diameter). In the discharge method, a pulse of $\sim$ 1 kV having 20–100-μs duration was applied to an electrode which located 10 mm downstream from the pulsed valve. In order to form 7-AzI–H_2O complex anions, a trace of H_2O (1–3 Torr) was added into the He carrier gas. The cluster anions were coaxially extracted by applying a pulsed electric field ($\sim$ 900 eV). After a 1.5-m flight path, the cluster anions were mass-selected by the TOF spectrometer and the target cluster anion was selected by pulsed deflection plates and decelerated to an energy of 10–20 eV by a potential elevator located in the magnetic bottle TOF spectrometer. The kinetic energy of electrons photodetached by the outputs of the other Nd^{3+}:YAG laser (Quanta-Ray, GCR-3) was analyzed by their TOF through a 70-cm drift tube. As well as the second/third/fourth harmonics of the Nd^{3+}:YAG laser (532/355/266 nm), the outputs from a Raman shifter with H_2 gas ($\sim$ 15 atm), which were 416.5 nm (1st Stokes of 355 nm), 338.9 nm (2nd Stokes of 266 nm), 309.3 nm (1st anti-Stokes of 355 nm), 299.1 nm (1st Stokes of 266 nm), 239.5 nm (1st anti-Stokes of 266 nm), and 218.9 nm (2nd anti-Stokes of 266 nm) were also used as the detachment laser. The photoelectron signal was accumulated into a multichannel scaler/averager (Stanford Research Systems, SR430). The energy of the photoelectron was calibrated by the measurement of photoelectron spectra of the Au^- anion, at three different wavelengths of 532 nm, 355 nm, and 266 nm, where the strong line attributed to the $^1S_0 \rightarrow {}^2S_{1/2}$ transition could be observed [26, 27]. The repetition rate was 10 Hz, and each spectrum typically represents an accumulation of 10 000–30 000 shots.

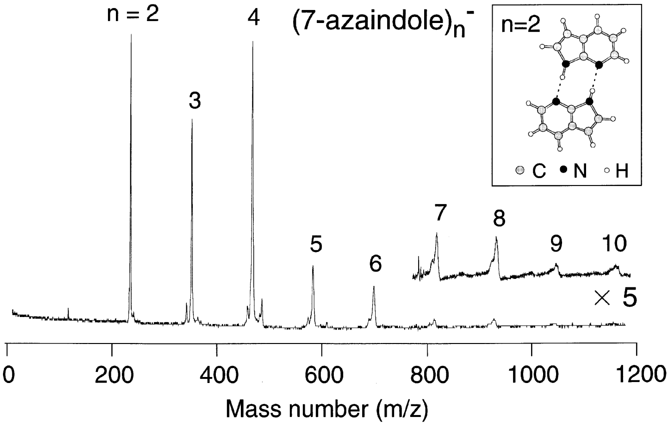

Fig. 1. TOF mass spectrum of 7-AzI cluster anions produced with the pulsed discharge nozzle; the horizontal axis is converted to be proportional to mass. The structure of the planar 7-AzI dimer is also shown at the point where two equivalent hydrogen bonds are formed.

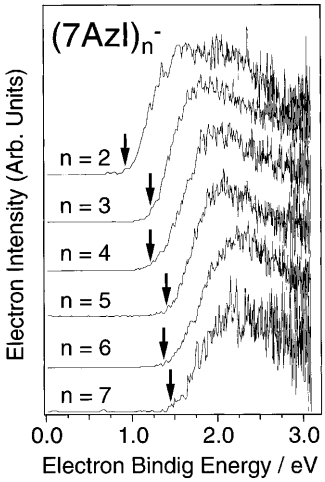

Fig. 2. Photoelectron spectra of 7-AzI cluster anions ($n = 2 - 7$) at 355 nm. Arrow shows the position of electron detachment threshold.

3 Results and discussion

The geometric and electronic features of 7-AzI cluster anions (Sect. 3.1) and their H_2O adducts (Sect. 3.2) will be discussed in terms of the use of mass spectrometry and photoelectron spectroscopy.

3.1 7-azaindole cluster anions

Figure 1 shows a TOF mass spectrum of $(\text{7-AzI})_n^-$ cluster anions produced with the pulsed discharge nozzle, which was almost the same as the mass spectrum obtained by the injection of electrons into the 7-AzI beam [24]. Analysis of the mass spectrum shows that no hydrogen atoms are lost, even with this discharge nozzle. This means that the $(\text{7-AzI})_n^-$ cluster anions were formed with negligible fragmentation even in the discharge nozzle. In both sources, no monomer anion was formed, suggesting that the 7-AzI molecule itself has a negative value of electron

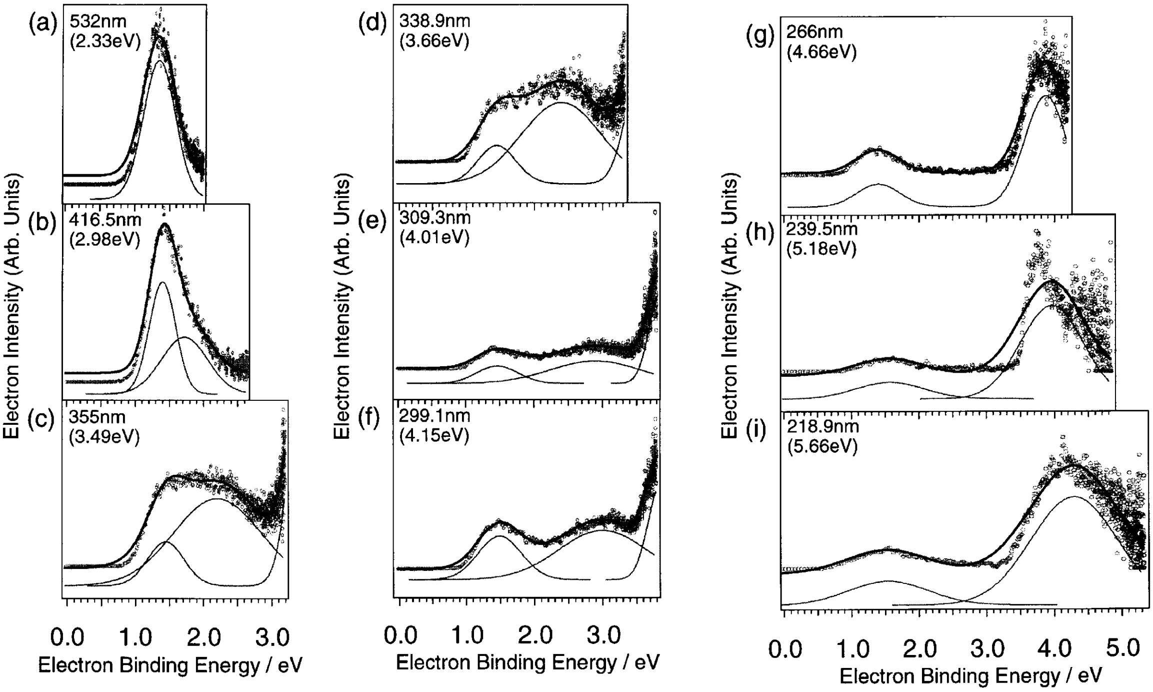

Fig. 3. Photoelectron spectra of 7-AzI dimer anions at various detachment wavelength: (a) 532 nm, (b) 416.5 nm, (c) 355 nm, (d) 338.9 nm, (e) 309.3 nm, (f) 299.1 nm, (g) 266 nm, (h) 239.5 nm, and (i) 218.9 nm. Gray dots show experimental data, and the gray narrow line shows each deconvoluted component fitted by a Lorentzian function. Solid line shows the best fitted curve for the experimental data.

Table 1. The threshold energy (E_T) of $(7\text{-AzI})_n(\mathrm{H_2O})_m$ cluster anions ($n = 2 - 7$) in eV

Cluster size (n, m)	E_T value[a)]
(2, 0)	0.88(12)
(3, 0)	1.20(11)
(4, 0)	1.20(10)
(5, 0)	1.38(13)
(6, 0)	1.36(18)
(7, 0)	1.48(16)
(1, 3)	0.48(16)
(1, 4)	0.75(12)
(1, 5)	0.99(12)
(1, 6)	1.17(14)

[a)] Numbers in parentheses indicate experimental uncertainties; 0.88(12) represents 0.88 ± 0.12.

affinity (EA). From $n = 2$ to $n = 10$, there appears a regular pattern in their abundance; from even n to odd $n+1$, there is an intensity gap. This intensity step indicates that the stability of the species is drastically changed before and after the step. Namely, cluster anions having even n are more stable that those having $n+1$. This result strongly implies that 7-AzI cluster anions are built up with a unit of 7-AzI dimer. In fact, it is well known that a 7-AzI molecule can form a very stable dimer with two equivalent hydrogen bonds. Since 7-AzI possesses both proton donor (N–H bond) and proton acceptor (N atom) sites, its dimer forms a planar structure via two hydrogen bonds. It seems reasonable, then, to presume the structure of the 7-AzI clusters to be a stacking of the 7-AzI dimer.

Figure 2 shows photoelectron spectra (PES) of the $(7\text{-AzI})_n^-$ cluster anions ($n = 2 - 7$) at the detachment energy of 3.49 eV (355 nm). In the PES spectra, the horizontal axis corresponds to an electron binding energy, E_b, which is defined as $E_\mathrm{b} = h\nu - E_\mathrm{k}$, where E_k is the kinetic energy of the photoelectron and $h\nu$ is the photon energy of the detachment laser. For the assignment of a photodetachment threshold energy, E_T, the slope of the first onset was extrapolated linearly to the baseline of the spectrum; the values are tabulated in Table 1. A downward arrow indicates the E_T value, and the E_T value corresponds to the upper limits of the adiabatic EA. The E_T value increases monotonically with the cluster size of n, and all the spectra exhibit similar bell-shaped envelopes without any reproducible fine structure. It should be noted that the EA of the neutral $(7\text{-AzI})_2$ shows an abrupt increase to 0.88 eV as compared to the negative EA of the monomer. Although the reason for this is unclear at the present stage, the network of the hydrogen bonding might work as a preferable site for electron trapping.

When the detachment wavelength was changed into a shorter one, the second peak was observed at the binding energy of 3.3 eV. Figure 3 shows the photoelectron spectra of $(7\text{-AzI})_2^-$ at various wavelengths of the detachment laser. This can be assigned to the transition into a triplet state of the neutral $(7\text{-AzI})_2$, and it has been revealed that the triplet state is located 2.4 eV above the neutral ground state of $(7\text{-AzI})_2$. Besides, an additional peak was observed between the first and the second peaks at the detachment of 420–300 nm (2.9–4.1 eV), depending on the detachment energy. In Fig. 3, gray dots show experimental data, and the gray line shows each deconvoluted component fitted by a Lorentzian function. The solid line shows the best fitted curve for the experimental data. From Figs. 3b to 3f, one component is conceivable along with the first peak fixed at $E_b = 1.35$ eV, but the component moves to the higher binding energy with the shorter detachment wavelength. The kinetic energy of the photoelectrons for the movable component is almost constant around $E_k = 1.4$ eV irrespective of the different detachment energy.

Furthermore, the laser power dependence of the peak shows that it originates from a one-photon process. This cannot be explained by usual photoelectron release through excitation into the electronic state of the corresponding neutral. It seems probable, then, that the additional peak is attributable to a delayed photoemission via an electronic excited state of the $(7\text{-AzI})_2^-$ anion, because the movable peak corresponds to the photoelectron release that occurs after a very rapid relaxation in the $(7\text{-AzI})_2^-$ anion.

As mentioned in the following section, the additional peak is indeed characteristic of the photoelectron spectra for the cluster anions containing two 7-AzI molecules. When two 7-AzI molecules are contained, the planar dimer is readily formed. This result suggests that the electronic excited state is located 2.9 eV above the ground state of the $(7\text{-AzI})_2^-$ anion, accompanying a very fast relaxation process, such as a proton-transfer reaction. Although there is no guarantee that the process via the excited state of the $(7\text{-AzI})_2^-$ anion should be a unique one, it seems reasonable that the $(7\text{-AzI})_2^-$ dimer exhibits the proton- transfer reaction in the excited state as well as the neutral dimer. For a definite explanation of the movable peak, the measurement of the electronic absorption for the $(7\text{-AzI})_2^-$ anion is indispensable, this is in progress in our group.

3.2 7-azaindole–water cluster anions

Figure 4 shows TOF mass spectra of 7-AzI–water cluster anions, $(7\text{-AzI})_n(\mathrm{H_2O})_m^-$, produced with the pulsed discharge nozzle, where the horizontal axis is converted to be proportional to mass. The $(7\text{-AzI})_n(\mathrm{H_2O})_m^-$ anions are hereafter expressed as $(n, m)^-$. From Figs. 4a to 4c, the concentration of water is qualitatively increased in the range of 0.1–3 Torr.

For the $(1, m)^-$ series, $(1, 3)^-$ appears as the first species, and larger cluster anions can clearly be observed. The EA of the neutral $(1, m)$ cluster becomes positive above $m = 3$. In Fig. 4c, in fact, the peaks of $(1, m)^-$ around 200 amu are distinctly shown for $m \geq 4$, although $(1, 3)^-$ is indiscernible. Figure 5 shows the photoelectron spectra of $(1, m)^-$ from $m = 3$ to 6 at 532 nm. All the spectra exhibit similar broad envelopes, and the threshold energy, E_T, increases monotonically with the number of H_2O molecules. The values of E_T are listed in Table 1. If one assumes that the EA increases proportionally to the number of H_2O molecules, the EA of 7-AzI in itself can roughly be estimated to be −0.5 eV. As reported previously [20], the high-resolution electronic spectra of the neutral $7\text{-AzI-}(\mathrm{H_2O})_n$, $n = 1-3$ clusters have revealed that the $7\text{-AzI-}(\mathrm{H_2O})_n$ clusters have planar structures, with water and the 7-AzI forming ring network structures. The ring chain, then, might act as an electron trapping in the $(1, m)^-$ clusters.

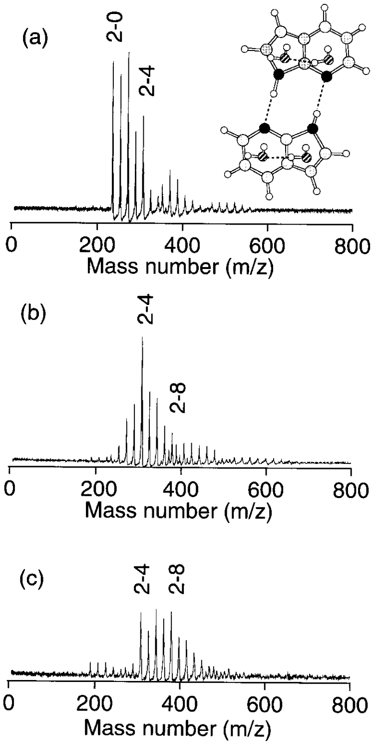

Fig. 4. TOF mass spectrum of 7-AzI–water cluster anions, $(7\text{-AzI})_n(\mathrm{H_2O})_m^-$, produced with the pulsed discharge nozzle; the horizontal axis is converted to be proportional to mass. From (a) to (c), the concentration of water is increased qualitatively. Peaks of the clusters are labeled according to the notation (n, m), which denotes the number of 7-AzI molecules (n) and water molecules (m), respectively. The presumed structure for $(2, 4)^-$ is shown in (a).

As shown in Figs. 4a–4c, moreover, $(2, 4)^-$ is prominently produced among the 7-AzI–water cluster anions, and $(2, 8)^-$ is observed as an intensity step, especially in Fig. 4b, although it overlaps with the $(3, m)^-$ series. Furthermore, even–odd alternation in peak intensity is weakly observed up to $(2, 8)^-$; species having an even number of H_2O molecules exhibit more intensity than those having an odd number of H_2O. The photoelectron spectra of $(2, m)^-$ exhibit similar bell-shaped envelopes to those of $(2, 0)^-$, suggesting that there is a core of $(7\text{-AzI})_2^-$ in $(2, m)^-$. Based on these features in the mass spectra and the photoelectron spectra, the results for the $n = 2$ series of $(7\text{-AzI})_n(\mathrm{H_2O})_m^-$ can be explained as follows: (1) Two 7-AzI exist as the dimer core having two equivalent hydrogen bonds; (2) each H_2O molecule is attached to every aromatic ring of $(7\text{-AzI})_2$ up to $m = 8$; and (3) every two H_2O form their dimers on a surface of 7-AzI molecule. It can reasonably be assumed that a T-shaped structure will be formed by the interaction between the H atom in H_2O and a π electron in the aromatic ring of 7-AzI, be-

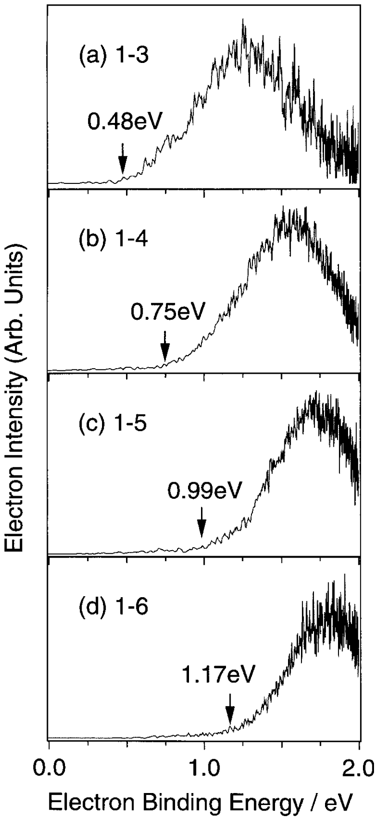

Fig. 5. Photoelectron spectra of 7-AzI–water clusters for $n = 1$ series of $(\text{7-AzI})_1(H_2O)_m^-$ $(m = 3-6)$ at 532 nm (2.33 eV). Downward arrow indicates the threshold energy of each cluster.

cause a similar structure has been reported in a study of benzene–H_2O [28]. The presumed structure for $(2,4)^-$ is shown in Fig. 4a. Although an H_2O molecule apparently prefers the proton donor (N–H bond) and proton acceptor (N atom) sites of 7-AzI rather than the aromatic rings, the occupation of both sites with the other 7-AzI leads the H_2O solvation into the ring sites. This is probably attributable to the high binding energy between two 7-AzI molecules, which is suggested by the larger red shift of the electronic excitation of the dimer than that of the 7-AzI–H_2O complex [20]. For the $(1,m)^-$ series, indeed, the mass distributions are relatively smooth; this is probably attributable to the favorable solvation into the proton donor and/or proton acceptor sites of 7-AzI. Interestingly, the movable peak appears also in the photodetachment of $(2,m)^-$; this is similar to the case of $(2,0)^-$ in Fig. 3. This result is consistent with the assumption that there is a core of $(\text{7-AzI})_2^-$ in $(2,m)^-$.

We are very grateful to Prof. Y. Ohshima (at the University of Kyoto) and Prof. Y. Endo (the University of Tokyo) for providing us details of the pulsed discharge nozzle. This work is supported by a program entitled “Research for the Future” (RFTF) of the Japan Society for the Promotion of Science (98P01203) and by a Grant-in-Aid for Scientific Research on Priority Areas from the Ministry of Education, Science, Sports, and Culture. A.N. expresses his gratitude to the Morino Foundation for Molecular Science for partial financial support.

References

1. P. Schuster, G. Zundel, C. Sandorfy (Eds.): *The Hydrogen Bonding Theory and Experiments* (North-Holland, New York 1976)
2. D.H. Levy: Ann. Rev. Phys. Chem. **39**, 197 (1980)
3. C.R. Cantor, P.R. Schimmel: *Biophysical Chemistry I* (Freeman, San Francisco 1980)
4. C.A. Taylor, M.A. El-Bayoumi, M. Kasha: Proc. Natl. Acad. Sci. USA **63**, 253 (1969)
5. K.C. Ingham, M.A. El-Bayoumi: J. Am. Chem. Soc. **96**, 1674 (1974)
6. K. Tokumura, Y. Watanabe, M. Udagawa, M. Itoh: J. Am. Chem. Soc. **109**, 1346 (1987)
7. H. Bulska, A. Chodkowska: J. Am. Chem. Soc. **102**, 3259 (1980)
8. W.M. Hetherington, R.H. Micheels, K.B. Eisenthal: Chem. Phys. Lett. **66**, 230 (1979)
9. D. McMorrow, T.J. Aartsma: Chem. Phys. Lett. **125**, 581 (1986)
10. R.S. Moog, S.C. Bovino, J.C. Simon: J. Phys. Chem. **92**, 6545 (1988)
11. K. Fuke, H. Yoshiuchi, K. Kaya: J. Phys. Chem. **88**, 5840 (1984)
12. K. Fuke, K. Kaya: J. Phys. Chem. **93**, 64 (1989)
13. C.-P. Chang, H. Wen-Chi, K. Meng-Shin, P.-T. Chou, J.H. Clements: J. Phys. Chem. **98**, 8801 (1994)
14. P.-T. Chou, H. Wen-Chi, C.-P. Chang, K. Meng-Shin: J. Phys. Chem. **99**, 11 994 (1995)
15. A. Douhal, S.K. Kim, A.H. Zewail: Nature **378**, 260 (1995)
16. L.A. Philips, D.H. Levy: J. Chem. Phys. **85**, 1327 (1986)
17. L. Yu, S.C. Foster, J.M. Williamson, T.A. Miller: J. Chem. Phys. **92**, 5794 (1990)
18. A. Held, D.W. Pratt: J. Am. Chem. Soc. **115**, 9708 (1993)
19. G. Berden, M.L. Meerts, M. Schmitt, K. Kleinermanns: J. Chem. Phys. **104**, 972 (1996)
20. A. Nakajima, M. Hirano, R. Hasumi, K. Kaya, C.C. Carter, J.M. Williamson, T.A. Miller: J. Phys. Chem. A **101**, 392 (1997)
21. O. Cheshnovsky, S.H. Yang, P.L. Pettiette, M.J. Craycraft, R.E. Smalley: Rev. Sci. Instrum. **58**, 2131 (1987)
22. G. Ganteför, K.H. Meiwes-Broer, H.O. Lutz: Phys. Rev. A **37**, 2716 (1988)
23. J.A. Walmsley: J. Phys. Chem. **85**, 3181 (1981)
24. A. Nakajima, F. Ono, Y. Kihara, A. Ogawa, K. Matsubara, K. Ishikawa, M. Baba, K. Kaya: Laser Chem. **15**, 167 (1995)
25. T. Ogata, Y. Ohshima, Y. Endo: J. Am. Chem. Soc. **117**, 3593 (1995)
26. H. Hotop, W.C. Lineberger: J. Phys. Chem. Ref. Data **4**, 539 (1975)
27. V.A. Esaulov: Ann. Phys. Fr. **11**, 493 (1986)
28. A.J. Gotch, T.S. Zwier: J. Chem. Phys. **96**, 3388 (1992)